Shock Waves in Gases*

W. C. Griffith and Walker Bleakney
Palmer Physical Laboratory, Princeton University, Princeton, New Jersey
(Received April 19, 1954)

This paper is in part a review but it also contains some original work. It deals with the manner in which shock waves are formed from finite compressions in gases and describes something of the structure of the shock front itself. The principal features of the behavior of shocks in reflection, refraction, and diffraction are discussed with particular attention given to anomalous observations and comparison with simple theories. Some results are given for shocks in real molecular gases showing relaxation effects. Quite a number of illustrations are included from the authors' own observations in the shock tube. The treatment is not exhaustive but covers many points likely to be of interest to teachers of physics.

INTRODUCTION

THE purpose of this paper will be to discuss some of the properties and effects of shock waves and their relation to sound waves. Everyone knows that the speed of sound in a gas is that speed at which small compressions are propagated by collisions between molecules. In fact, the speed of sound is approximately equal to the average molecular velocity. Shocks, on the other hand, are characterized by a large increase in pressure within a few mean free paths and advance at supersonic speeds. Explosions and lightning are two familiar sources of shocks. In both cases a region of high pressure is suddenly created from which a shock travels outward through the surrounding air. Since energy must be spread over an ever increasing surface as the shock expands its strength will diminish both from the expansion and from viscous dissipation. Eventually the shock will decay into a sound wave.

We shall first describe some of the properties of small amplitude sound waves. An extension of the theory then leads to the prediction that large amplitude waves tend to steepen on the front side and decline in back. When viscous effects are sufficiently small theory shows that the front of a continuous compression wave will eventually become infinitely steep. In the physical sense we say that a shock has formed. We shall then develop various relations pertaining to shocks and discuss their behavior in reflection, refraction, and diffraction. A device called the shock tube for producing them in the laboratory under controlled conditions will be described. Finally, mechanisms for the eventual decay of shocks into sound waves are considered.

* Part of the work described in this paper was supported by an U. S. Office of Naval Research contract.

PROPAGATION OF SOUND WAVES

The speed of sound in a gas may be found by applying the principles of conservation of mass and momentum to the medium and assuming that the compressions produced by passage of the sound are isentropic.[1] A wave equation for the variation in pressure results,

$$a^2\partial^2 p'/\partial x^2 = \partial^2 p'/\partial t^2. \tag{1}$$

Here p' is the change in pressure from ambient at a point x and time t and a is the velocity of sound given by

$$a^2 = dp/d\rho, \tag{2}$$

where it is understood that the derivative of pressure p with respect to density ρ is to be taken with the entropy constant. Many gases behave like an ideal gas for which

$$p = \rho RT, \tag{3}$$

R is the gas constant per unit mass, and T the temperature. If the specific heats C_p and C_v are constant and their ratio denoted by $\gamma = C_p/C_v$ the speed of sound may be expressed as

$$a^2 = \gamma RT. \tag{4}$$

This equation also gives the speed of a finite rarefaction wave advancing into a gas at rest,[2]

[1] See for instance W. F. Durand, *Aerodynamic Theory* (Verlag Julius Springer, Berlin, 1934), Vol. III, p. 210.
[2] I. I. Glass, J. Aeronaut. Sci. 19, 286 (1952).

TABLE I. Velocity of sound in ft/sec at 20°C for air, argon, carbon dioxide, and nitrous oxide obtained by four methods: (1) continuous sinusoidal waves, (2) extrapolation of weak shock velocities, (3) finite rarefactions, and (4) calculation from Eq. (4). In addition the values of γ at 20°C computed from the specific heats are included.

Gas	Air	A	CO_2	N_2O
1. C. W.[a]	1126	1048	877	
2. Weak shock	1126		874	875
3. Rarefaction[a]	1126	1045	874	
4. $\sqrt{(\gamma RT)}$	1126	1046	877	872
5. γ	1.400	1.667	1.290	1.275

[a] Values for the velocity of continuous sound waves from the literature and the speed of a rarefaction wave are given in reference 2 together with probable errors. The data for weak shocks are original, and the estimated accuracy is ±1 for air and ±2 for the other gases.

predicts the asymptotic speed of a shock as the shock becomes vanishingly weak, and applies to gases with variable specific heat as long as Eq. (3) is an adequate equation of state. All of these methods have been used to determine the speed of sound in several different gases. It is interesting to compare the various experimental results with one another and with the theoretical value. Table I summarizes the data for four common gases, air, argon, carbon dioxide, and nitrous oxide. The agreement is quite gratifying in view of the variety of methods involved.

An appreciation of the extremely small amplitudes associated with the propagation of sound may be gained by noting that the pressure fluctuations in the loudest sound that is not actually painful is one thousandth of atmospheric pressure. The faintest sound the ear can detect is a variation of about 3×10^{-10} atmosphere pressure. Since the pressure amplitude of a spherically expanding wave drops off only inversely with distance, it is easy to see why sounds may be heard at great distances from their origin. Of course, accidental focusing by wind and temperature gradients may greatly increase this range.

In spite of the small amplitudes of audible sound waves there is a tendency for the crests to move slightly faster than the troughs since they are at a slightly higher temperature. Thus a sinusoidal wave will become distorted after traveling some distance. Viscosity acts to limit such distortion and a steady condition is reached in which the two effects just balance one another.

This problem has been studied in some detail.[3] When the simplifying assumption of infinitesimal amplitudes is dropped and the existence of viscous forces taken into account, a more complicated differential equation than the wave equation results whose solution may be expressed in terms of a Fourier series. The stable wave shape even in a one-dimensional problem is found to be a function of the amplitude. There is therefore no fixed wave shape but a continuously varying one leading finally to a sine wave when most of the energy has been dissipated. As an example the wave shape for a thousand-cycle plane wave with $p'=10^{-5}$ atmosphere has been computed numerically[3] and is shown in

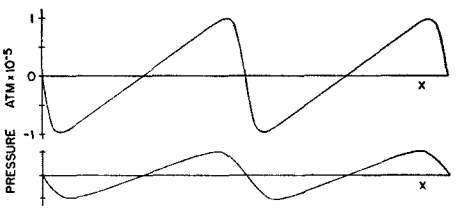

FIG. 1. Calculated wave shape for a thousand cycle note having an amplitude of 10^{-5} atmos and the same wave when the amplitude has decreased by half.

Fig. 1 along with the shape of the same wave when its amplitude has decreased by half.

FINITE COMPRESSION PULSES

A single compression wave of finite size may be generated in an imaginary experiment as follows: a tight-fitting piston in a long horizontal tube is accelerated to the right for a short time and then brought to rest again a distance L from its original position. A compression wave will advance through the air ahead of the piston and move every particle a distance L to the right. Initially the wave will have some shape as shown in Fig. 2a. Since each part of the wave advances with the local velocity of sound the same sort of steepening will occur with time as did in the large amplitude sound waves. For the moment let us neglect the influence of dissipation and follow the changes in wave shape arising from temperature effects alone.

Riemann[4] studied this problem many years ago and found that the disturbance travels in such a way that any point B with pressure p and particle velocity v advances with the speed

[3] R. D. Fay, J. Acoust. Soc. Am. **3**, 222 (1931).

[4] B. Riemann, Göttingen Abhandlungen **8**, 43 (1860).

$v+a$, where a is the local speed of sound. In terms of the speed of sound a_1 ahead of the compression B travels with speed $a_1+(\gamma+1)v/2$.[5] If one has the velocity profile at a given time $t=0$ (Fig. 2b), then the profile at a later time Δt may be found by advancing each point of the wave front a distance $[a_1+(\gamma+1)v/2]\Delta t$. This construction has been carried out in Fig. 2c. It is evident that after a time $t=2/[(\gamma+1)(dv/dx)_{t=0}]$ a vertical tangent will be reached as in Fig. 2d.

An experimental verification of the foregoing theory has been obtained in the shock tube with the aid of an interferometer. Three pictures in Fig. 3 show how the density in a compression wave varies with time. Suffice it to say for the moment that the vertical displacement of a given fringe is directly proportional to the density. We conclude that an infinite slope in the theoretical solution corresponds to a shock in

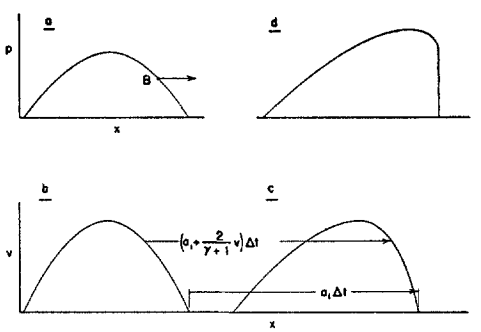

FIG. 2. Construction showing how a compression wave steepens into a shock according to Riemann's theory. When a vertical tangent is reached we say that a shock is formed.

real life. In the next section we shall investigate the properties and structure of shocks by means of the conservation equations.

SHOCK WAVES

The conservation equations for a fluid enable us to draw many conclusions about the behavior of shocks without knowing anything about their structure. For an observer riding on a shock in one-dimensional steady flow let us use the symbols p_1, v_1, ρ_1, and h_1 to give the values of pressure, velocity, density, and enthalpy at a point far enough ahead of the shock for conditions to be uniform. Similarly the subscript 2 will denote equilibrium conditions behind the shock. Then the equations are:

conservation of mass

$$\rho_1 v_1 = \rho_2 v_2; \tag{5}$$

momentum

$$p_1+\rho_1 v_1^2 = p_2+\rho_2 v_2^2; \tag{6}$$

energy

$$h_1+v_1^2/2 = h_2+v_2^2/2. \tag{7}$$

In general the enthalpy is a fairly complicated function of temperature so that these three equations and the equation of state are difficult to solve. For the special case of an ideal gas with constant specific heat, however, $h=c_pT=\gamma p/\rho(\gamma-1)$. If the velocities are eliminated an equation between the pressure and density ratios across the shock is obtained,

$$\frac{\rho_2}{\rho_1}=\left[1+\frac{\gamma+1}{\gamma-1}\frac{p_2}{p_1}\right]\Big/\left[\frac{\gamma+1}{\gamma-1}+\frac{p_2}{p_1}\right]. \tag{8}$$

This relation was found independently by Rankine and Hugoniot in the last century[6] and is named after them. It is applicable to monatomic gases over a wide range of temperatures and works well for air up to about 500°K. Above this range appreciable vibrational energy is present so c_p is no longer constant.

The symmetry of Eq. (8) suggests that rarefaction shocks might also exist in nature. These may be shown to lead to a decrease in entropy,

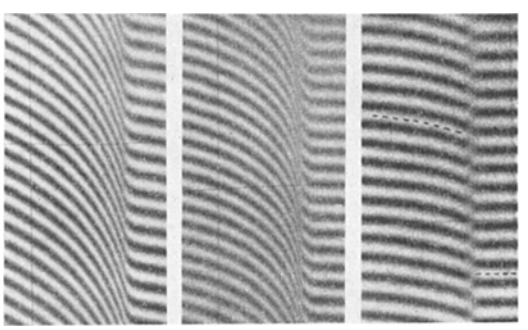

FIG. 3. Fringe pattern obtained with an interferometer of three stages in the formation of a shock from a continuous compression. The wave is traveling toward the right. The vertical position of a given fringe is proportional to the density at that point. In the last picture a jump of seven fringes occurs.

[5] Reference 1, Vol. 3, p. 216.

[6] W. J. M. Rankine, Phil. Trans. Roy. Soc. 160, 277 (1870). H. Hugoniot, J. école polytech (Paris) Nos. 57–59 (1887–89).

however, and must be ruled out by the second law of thermodynamics.[7]

If velocities are measured in units of the local speed of sound several useful relations assume a specially simple form. With the same assumptions as before and the Mach number M defined as v/a, the shock density and pressure ratios are

$$\rho_2/\rho_1=1\Big/\left[\frac{2}{(\gamma+1)M_1^2}+\frac{\gamma-1}{\gamma+1}\right], \tag{9}$$

$$p_2/p_1=1+\frac{2\gamma}{\gamma+1}(M_1^2-1). \tag{10}$$

Both are seen to be monotonically increasing functions of the shock speed. The speed becomes infinitely great for an infinite pressure ratio but the density ratio approaches a finite value of $(\gamma+1)/(\gamma-1)$, which is 4 for the monatomic gases.

The Mach number of the flow leaving the shock can be derived from the preceding relations and is given by

$$M_2^2=\frac{v_2^2}{a_2^2}=\frac{1+\frac{\gamma-1}{\gamma+1}(M_1^2-1)}{1+\frac{2\gamma}{\gamma+1}(M_1^2-1)}. \tag{11}$$

Since M_1 is always greater than one for a shock to exist the numerator is always less than the denominator and we may conclude that v_2 is always less than a_2. This property is essential to the stability of a shock with respect to slight disturbances for it will be able to catch any signal that may run ahead and will also be caught by any that get behind.

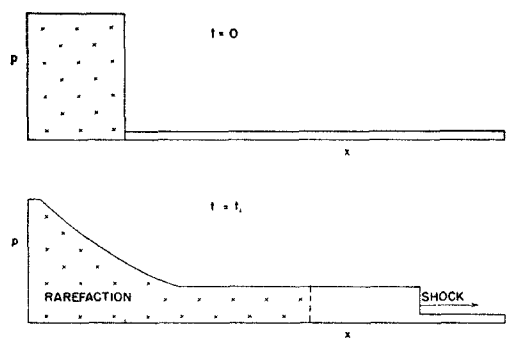

FIG. 4. Schematic drawing of the pressure distribution in a shock tube before and just after the diaphragm is burst. As an aid in visualizing the flow produced, the volume occupied by particles originally in the high pressure end is cross-hatched.

THE SHOCK TUBE

To investigate the properties of these shocks it is desirable to be able to produce them at will in the laboratory. A device for doing this is called the shock tube. It consists of a long pipe divided into two sections, one of which at the time of initiation is at high pressure and so propagates a compression into the other which rapidly becomes a shock. The high-pressure region may be created in several ways. It may be built up mechanically behind a diaphragm which is broken at the moment of initiation. Or a large change in pressure may be induced by such means as chemical explosion, electric discharge or exploding wires. The shock strength is controlled by the starting pressure and temperature ratios.

Once the shock is formed it moves with constant velocity through the medium ahead and is followed by a column of gas of uniform state traveling with velocity v_1-v_2 relative to the laboratory. The pressure distribution before and shortly after a cellophane diaphragm is punctured is shown in Fig. 4. The flat-topped shock will persist until it reaches the end of the tube or is caught by the rarefaction which sweeps into the high pressure gas and is reflected from the back end of the tube. Rather complete details on the theory of the shock tube may be found in the literature.[8–13]

The Princeton shock tube is 4 in. by 18 in. in cross section and 38 ft long. Experience has

[7] H. Liepmann and A. Puckett, *Aerodynamics of a Compressible Fluid* (John Wiley and Sons, Inc., New York, 1947), p. 40.

[8] Bleakney, Weimer, and Fletcher, Rev. Sci. Instr. **20**, 807 (1949).

[9] J. Lukasiewicz, "Shock tube theory and applications," National Aeronautical Establishment of Canada, Report 15, 1952.

[10] P. W. Geiger and C. W. Mautz, "The shock tube as an instrument for the investigation of transonic and supersonic flow patterns," Engineering Research Institute, University of Michigan, 1949.

[11] Glass, Martin, and Patterson, "A theoretical and experimental study of the shock tube," University of Toronto Institute, Aerophysics Report 2, 1953.

[12] R. K. Lobb, "On the length of a shock tube," University of Toronto Institute of Aerophysics Report 4, 1950.

[13] Resler, Lin, and Kantrowitz, J. Appl. Phys. **22**, 878 (1951).

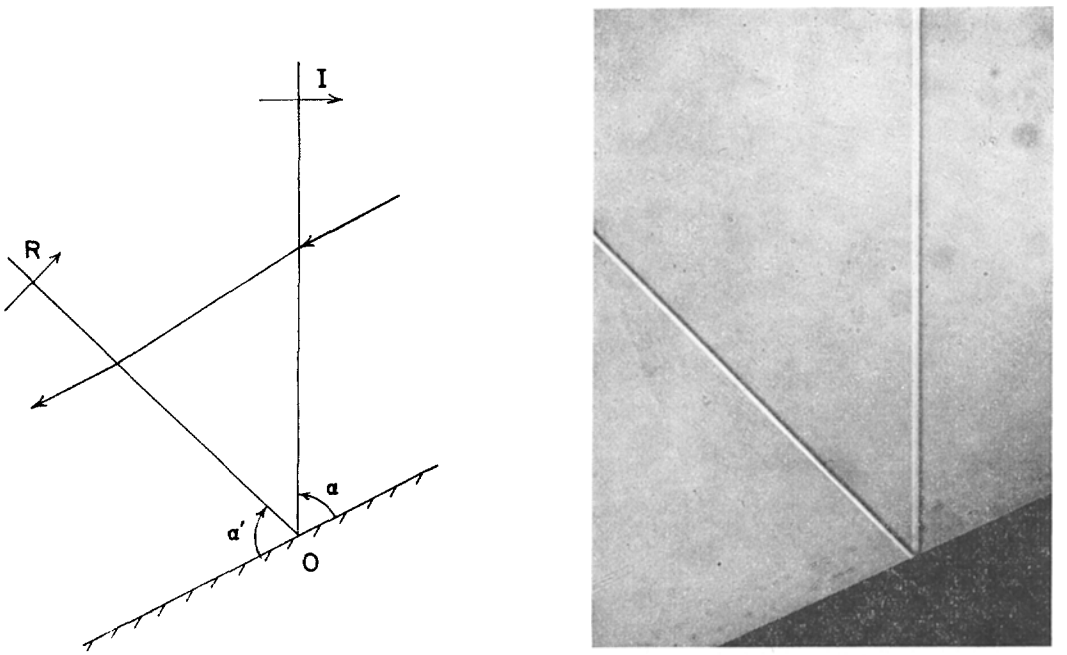

(a) (b)

FIG. 5. Shadow picture showing reflection of a shock of Mach number 1.034 from a solid wall. The incident shock sets the air in motion. Relative to the point O a given particle follows the path shown in the construction on the left.

shown that the shock has sufficient time to become fully formed after traveling about ten tube diameters. Shock velocities are measured by noting the time of passage between two schlieren light screens a known distance apart. As the shock passes each screen the beam is momentarily deflected into a photocell. The pulses from the photocells are fed into an oscilloscope and recorded photographically on a drum camera. The pulse from the second light screen also actuates an adjustable electronic delay circuit which triggers a one microsecond spark. Since the shock strength is very accurately repeatable from one shot to the next a series of pictures may be obtained showing the development of any event.

The flow patterns may be observed by interferometer, schlieren, or shadow photography. Shadow pictures are the easiest to get and give the clearest information on the position of shocks. For quantitative information an interferometer is superior since the shift of fringe position is directly proportional to the density change in two-dimensional flow. By geometrical optics it can be shown that schlieren gives a measure of density gradient while shadow is sensitive to the second derivative of density. As an example the shadow picture in Fig. 5 and interferograms in Fig. 6 taken with white and monochromatic light show a shock of Mach number 1.034 being reflected from an incline. Careful measurements reveal that the apparent shock thickness in Fig. 5 is a result of the 1-μsec spark duration measured with a rotating mirror. In a later section we shall see that the actual thickness is $\sim 10^{-5}$ inch. The small number of fringes visible in the white light picture enable us to identify fringes on either side of the shock. If the shift in fringe position δ is measured in units of the original fringe spacing, the density change is given by Eq. (12) where λ is the wavelength of light, n_s is the index of refraction and ρ_s the density of the gas at STP, and l is the width of the test section,

$$\rho_2 - \rho_1 = [\lambda \rho_s / l(n_s - 1)]\delta. \qquad (12)$$

Since the interferometer and the light screens provide two independent methods of measuring shock strengths we may make an experimental check of the Rankine-Hugoniot relation [Eq.

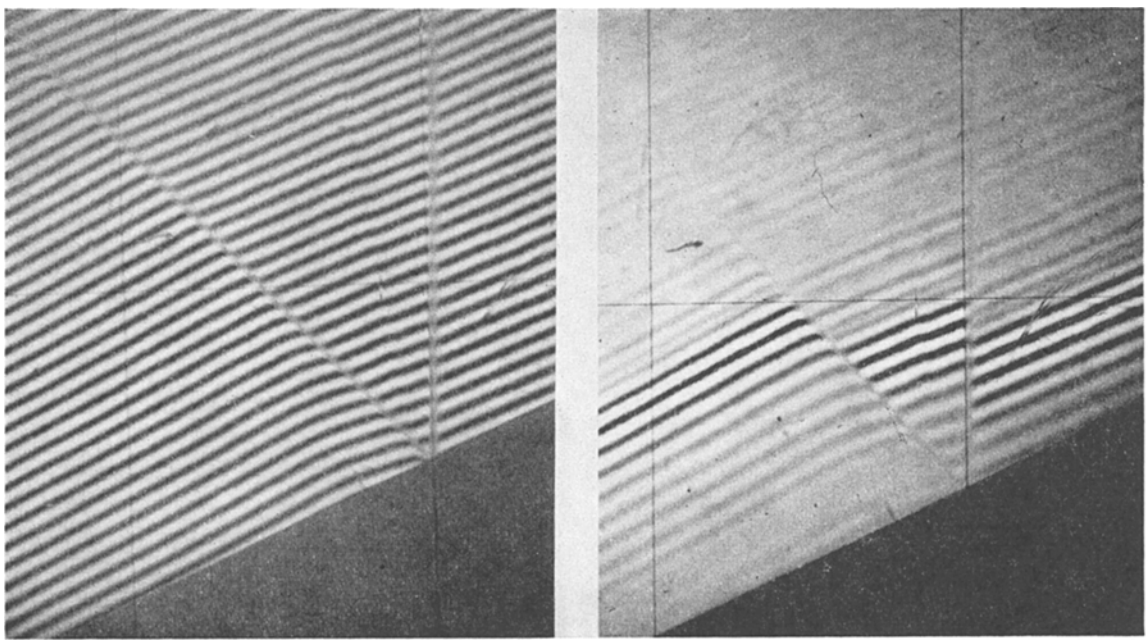

FIG. 6. Interferograms taken with monochromatic and white light of the same shock shown in Fig. 5. The small number of fringes visible in the white light picture makes it possible to find the density change across a shock.

(8)], or, as some prefer to look at it, a check on the accuracy of our measurements. Shock pressure ratios for air have been computed from interferometer data using Eq. (8) and from velocity measurements using Eq. (10) for a large number of experiments. In each of nine arbitrary intervals between $p_1/p_2=0.95$ and 0.15 the average values agree to one part in a thousand, corresponding to relative accuracies of 0.1 percent for weak shocks and 0.7 percent for the stronger ones. Above this range of shock strengths, $M>2.4$, the temperature becomes high enough to excite appreciable molecular vibrational motion in O_2 and N_2 so that γ is no longer constant. Solution of the flow equations for such cases will be discussed later.

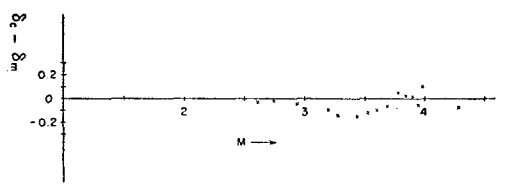

FIG. 7. Direct experimental test of the Rankine-Hugoniot relations for argon. The calculated fringe shift δ_c is obtained by these relations from the shock velocity. The difference between the resulting value and that actually measured with the interferometer, δ_m is plotted as a function of shock Mach number.

Argon, on the other hand, has such a large electronic excitation energy that its behavior should agree with prediction of the present theory up to very high temperatures. Accordingly, a series of pictures have been taken in argon with shock Mach numbers between 2.6 and 4.3. The large pressure ratio required to generate the strongest shocks limits the pressure in the channel to about 10 mm-Hg. The corresponding fringe shift is slightly less than two so that measurements with the interferometer become decreasingly sensitive. A meaningful comparison of speed and fringe measurements may be made by computing the fringe shift we would expect from the shock velocity. This has been done for fifteen experiments and the results are plotted in Fig. 7. Here the fringe shift computed from the velocity minus that actually measured is shown as a function of Mach number. The average of all values is $-1/20$th fringe and it may be seen that no point differs from this average by more than 1/15th of a fringe. This is well within our estimated error from all causes which we have previously taken as 1/10th fringe. So far as we know these results in air and argon are the best direct experimental verification of the validity

of the assumptions made in deriving the Rankine-Hugoniot relation. It is, of course, just the result we expected to get.

SHOCK INTERACTIONS

Probably the simplest problem of shock interaction that one can formulate is that analogous to Snell's law for reflection and refraction. For shocks the angle of incidence and reflection will in general not be equal because the incident shock produces an increase of entropy of the gas so that the reflected shock must travel through a medium having a different thermodynamic state. The problem of reflection on a wall may be formulated as follows: For a given shock strength and angle of incidence what reflected waves will leave the gas flowing parallel to the wall? In Fig. 5 the incident shock I strikes the wall at an angle α to produce a reflected shock R at the angle α'. Consider a coordinate system in which the point of intersection O is at rest. The change in components of velocity normal to the shocks can be found from Eqs. (9) and (11), while the tangential components of velocity are unaffected. Polachek and Seeger[14] solved the

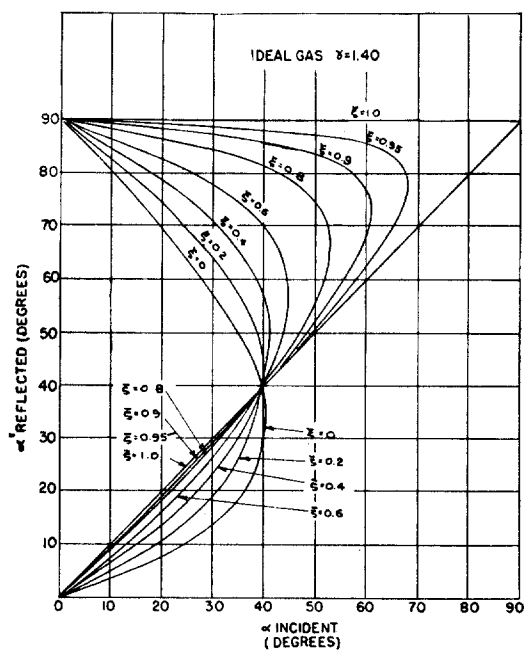

FIG. 8. Theoretical solution for the reflected shock angle α' as a function of the angle of incidence α and the shock strength $\xi = p_1/p_2$.

[14] H. Polachek and R. Seeger, "Regular reflection of shocks in ideal gases," Explosive Research Report No. 13, Bureau of Ordnance, U. S. Navy Dept., 1944.

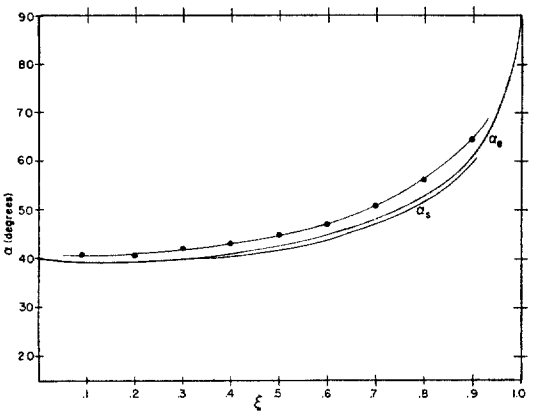

FIG. 9. Comparison of theory and experiment for the transition between two-shock (regular) reflection and three-shock (Mach) reflection. α_e is the angle above which no two-shock solution exists in Fig. 8, α_s is the angle of incidence for which the outflow from the reflected shock becomes sonic, and α_o is the experimentally observed transition angle (upper curve).

resulting set of equations for α' subject to the condition that the two shocks deflect the flow equal amounts but in opposite directions. Their results are shown in Fig. 8 for eight shock strengths. The parameter ξ is defined as the ratio of pressure ahead of a shock to that behind, $\xi = p_1/p_2$, so that $\xi = 1$ gives the sonic case and $\xi = 0$ corresponds to an infinitely strong shock. Two features of these curves are of special note: only for sufficiently small values of α, $\alpha < \alpha_e$, do any solutions exist and below these extreme values two possible reflected waves can occur. Of the two, that for smaller α' gives the weaker reflected shock.

One further limitation is placed on the region of two-shock or regular reflection by the relations between the curvatures of shocks and streamlines where they cross.[15] Above a limiting angle of incidence the reflected wave is curved throughout its length and difficulties are encountered in meeting the boundary conditions at the wall. As a consequence the flow behind the intersection must be at least sonic for the simple two-shock idea to apply. The angle for which the outflowing air becomes sonic with respect to O is designated by α_s in Fig. 9 where it is plotted as a function of ξ together with the extreme angle α_e.

Extensive experiments have been carried out

[15] A. H. Taub, Ann. Math. 58, 501 (1953).

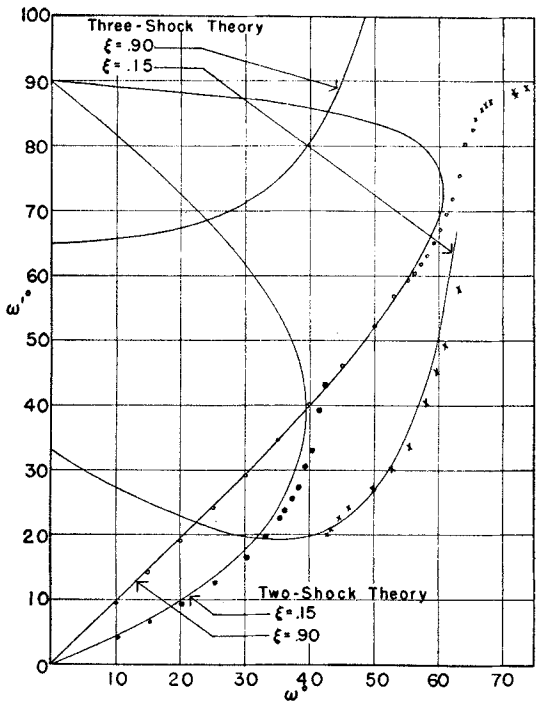

FIG. 10. Experimental and theoretical values for the reflected shock angle α', or for Mach reflection ω', as a function of the angle of incidence for one strong shock strength, $\xi=0.15$, and one weak shock, $\xi=0.9$. The circles indicate points where regular reflection is observed and the x's are for Mach reflection. Here, as is usual practice, the coordinates are $\omega=\alpha-\chi$ and $\omega'=\alpha'+\chi$ (see Fig. 12), where χ is zero for regular reflection. The angle between the incident shock and the incoming flow relative to the intersection is therefore ω.

by Smith,[16] and his measurements show good agreement between experiment and the solution leading to the weaker reflected shock. Results for $\xi=0.15$ and 0.9 are shown in Fig. 10. It might be mentioned that in steady supersonic flow past a wedge the weaker shock is also the one commonly observed. No proof of greater stability for the weaker wave has been found as yet.

When the angle of incidence exceeds the value for which any regular reflection exists a new and quite different pattern is observed experimentally as shown in Fig. 11.[17] Mach reflection, named for Ernst Mach who first observed the effect,[18] shows the incident and reflected shock meeting some distance from the wall with a third shock extending from the point of intersection to the wall. This third shock will be called the Mach stem and the point of intersection the triple point.

An additional discontinuity extends back from the triple point. This is a slipstream separating the gas which has passed through the incident and reflected shocks from that which has gone through the Mach stem. The entropy changes are slightly different so that the requirement of equal pressures if the streamlines are to be parallel gives slightly different particle velocities. The magnitudes are such that the gas above flows away from the triple point faster than that below.

The use of a symmetrical wedge rather than an incline on a plane reduces the disturbing effect of the viscous boundary layer at the solid surface. Since there is no dimension inherent in the configuration it seems reasonable to suppose, and experiment bears this out, that the pattern grows similar to itself in time. That is, the flow is pseudostationary and the three independent coordinates x, y, t reduce to two:

1→

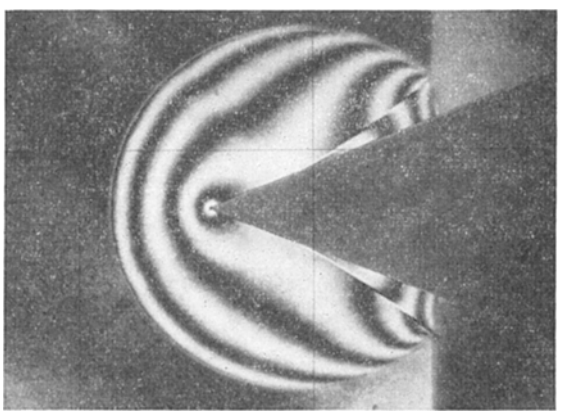

FIG. 11. Mach reflection of a shock from a symmetrical wedge. $\xi=0.42$. For this picture the interferometer is adjusted so that a uniform field exists when no disturbances are present. Contours of equal brightness then become lines of constant density.

[16] L. G. Smith, "Photographic investigations of the reflection of plane shocks in air," OSRD Report No. 6271, 1945.

[17] The interferogram shown in Fig. 11 was obtained using a different adjustment of the interferometer from that for Fig. 6. In this case the mirrors are set exactly parallel to give uniform interference over the entire field when no disturbances are present. When the shock arrives regions of equal density will change the optical path length equally and appear as light and dark fringes. Thus the density field is presented directly. This method has the disadvantage that the contours cannot be labeled without doing additional experiments but will be used here frequently because it illustrates features of the flow so vividly.

[18] E. Mach, Akad. Wiss. Wien 77, 819 (1878).

x/t, y/t. This was first suggested by von Neumann.[19] Even with this reduction in the number of variables the mathematical problem is so formidable that no general solution for the flow field in Mach reflection has been discovered. Several proposals have been put forth to treat special cases and a representative example will be discussed in the following paragraphs.

If the flow is pseudostationary the triple point T travels along a straight line through the corner C making some angle χ with the surface as in Fig. 12. By letting the flow proceed long enough any degree of magnification desired of the region near the triple point can be obtained. No singularities in shock curvature have been observed in the pictures. This suggests that conditions are continuous in all of the angular domains around T bounded by the four discontinuities, and it seems plausible to assume that the shocks can be treated as straight as one approaches arbitrarily close to T. To an observer riding with the triple point the three-shock situation is thus similar to the two-shock problem investigated before. Here the condition of flow parallel to the wall is replaced by the requirement that the velocities behind the triple point be parallel and the pressures equal. von Neumann has solved the resulting equations in terms of the shock angles $\omega=\alpha-\chi$ and $\omega'=\alpha'+\chi$ relative to the line at angle χ. The resulting values of the three-shock solution are plotted in Fig. 10 (where for regular reflection $\chi=0$ and $\alpha=\omega$) for $\xi=0.15$ and 0.9. Agreement with experiment is fair for the strong shocks ($\xi=0.15$) but is poor for the weak case. This result is surprising in view of the success of the two-shock theory. An additional problem is that of understanding the persistence of two-shock reflection beyond the theoretical limit as illustrated in Fig. 9. The curve α_0 shows the experimental points where χ becomes zero, representing the transition between Mach and regular reflection. In summary, we may say that we have a local theory for the angles at the intersection which work for regular reflection below α_s and for Mach reflection above α_0 for strong shocks. Outside this range clearcut discrepancies exist which still need to be explained.

[19] J. von Neumann "Oblique reflection of shocks," Exptl. Res. Rep. No. 12, Bureau of Ordnance U. S. Navy Department, 1943.

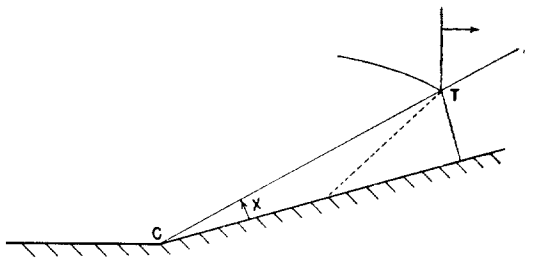

FIG. 12. Construction showing how the angle χ is defined. When the flow is pseudostationary the triple point T moves in such a way that χ remains constant.

The only complete solutions of the reflection problem discovered so far are restricted either to nearly glancing incidence ($\alpha=90°$) or to nearly head on reflection ($\alpha=0°$). Since experiments must be made at an angle at least 5° different from these limits in order to detect anything a problem of interpretation arises which can be resolved either by extrapolating experimental data to zero angle or by making a second-order correction to the theory. Four papers[20–23] dealing with solutions of this type agree quite well with experiment.[24,25] One such case will be reviewed here.

Ting and Ludloff[23] have reported a method which they used to find the flow field when an incline is struck by a shock strong enough to produce supersonic flow relative to the corner. (For air this requires that p_2/p_1 be greater than 5.) The mathematical approach used has been explained more fully elsewhere.[24] White[25] has compared their results for one shock strength with his measurements. Figure 13 shows the theoretical and experimental results for a shock of strength $\xi=0.137$. Evidently there is good agreement in both the shape of the pattern and the quantitative values of the density contours. Such discrepancies as exist can be ascribed to the finite angle used in the experiment.

Knowledge about shock refraction is in a very

[20] V. Bargmann, "On nearly glancing reflection of shocks," OSRD, No. 5171, 1945. See also reference 24.
[21] M. J. Lighthill, Proc. Roy. Soc. (London) **A198**, 454 (1949).
[22] M. J. Lighthill, Proc. Roy. Soc. (London) **A200**, 554 (1950).
[23] L. Ting and H. F. Ludloff, J. Aeronaut. Sci. **18**, 143 (1951).
[24] Fletcher, Taub, and Bleakney, Revs. Modern Phys. **23**, 271 (1951).
[25] D. R. White, "An experimental survey of the Mach reflection of shock waves," Proc. Second Midwestern Conference on Fluid Mechanics, Ohio State University, 1952.

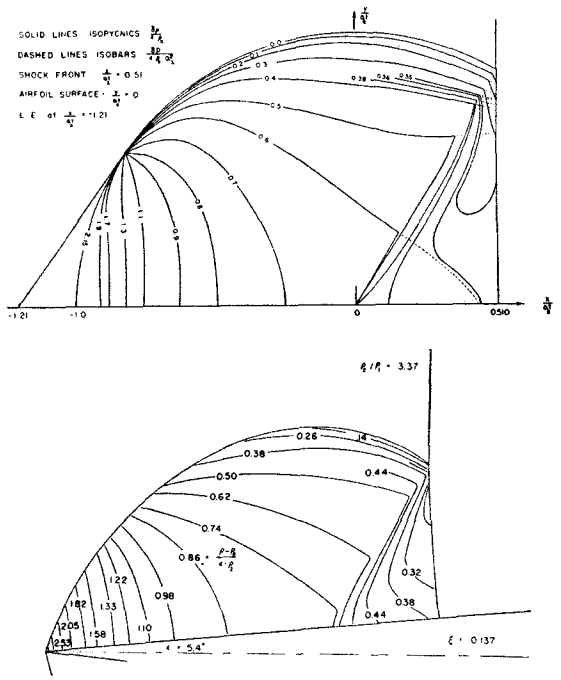

FIG. 13. Comparison of Ting and Ludloff's solution (above) with White's experimental result (below) for a shock of Mach number 2.53 striking a small incline of 5.4°. The solid lines are contours of constant density.

much more primitive state than for reflection because of the multiplicity of solutions obtained theoretically and experimental difficulties in forming a suitable interface between two gases. Again let us study "regular" refraction first where only the possibility of straight shocks is considered. In Fig. 14 the line OD represents the boundary between the two gases having specific heat ratios γ_1, γ_5, and velocities of sound a_1, a_5. The incident, reflected, and transmitted waves are represented by I, T, and R, respectively. Five quantities are necessary to specify a problem completely; the incident shock strength ξ, its angle of incidence α, the ratio of sound speeds a_1/a_5, and γ_1 and γ_5. Relative to the point of intersection O the boundary conditions are that the flow direction and pressure behind R be the same as behind T. The boundary may be deflected to some new direction OB. Solutions of the resulting equations for several combinations of gases have been obtained by Taub[26] and by Polachek and Seeger[27] with the aid of electronic computers. Polachek and Seeger also considered the possibility that the reflection R be an expansion fan centered at O rather than a shock.

Several physical limitations must be placed on the mathematical solutions in order that the results be meaningful. Even when this is done, however, more than one choice often remains and one must apparently rely on experiment to pick the correct branch. A special argument may be made for those branches of the solution which approach the well verified acoustical version of Snell's law, $\sin\alpha/\sin\alpha'' = a_1/a_5$, for vanishing shock strength and the head-on refraction of finite shocks where one-dimensional solutions may be found easily. Until experiments are carried out, however, such discussions must be of a purely speculative nature.

In addition to the existence of an extreme angle α_e beyond which no solutions of regular refraction exist at all, the following possibilities must be considered as α varies; (a) the flow velocity normal to the reflected wave must be at least sonic, i.e., α is limited by some value which we shall denote as α_s; (b) a reflected shock may vanish and become a reflected rarefaction instead, the transition occurring at $\alpha = \alpha_t$; (c) for the transmitted shock to exist the velocity of the point of intersection must be supersonic with respect to the lower medium (gas 5), limiting α to values less than α_i. Extra complications will arise if the outflow is not supersonic in both media.

A single example will be included here; that of a shock striking an air-methane interface. For

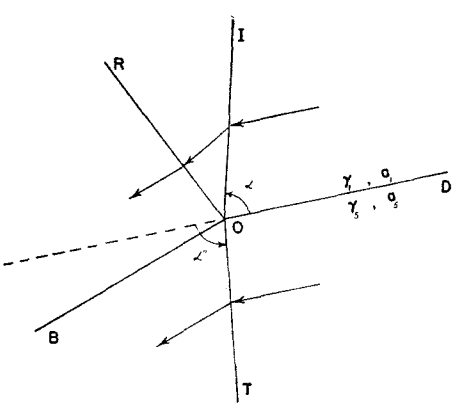

FIG. 14. Pattern of "regular" refraction at the interface OD between two gases. Flow directions relative to point O are shown.

[26] A. H. Taub, Phys. Rev. 72, 51 (1947).
[27] H. Polachek and R. Seeger, Phys. Rev. 84, 922 (1951).

other cases the reader is referred to the papers already cited. For normal incidence ($\alpha=0$) a shock is transmitted through the methane and a rarefaction reflected into the air. This occurs because the particle velocity behind the shock in methane is greater than that of the air passed over by the incident shock so the air must accelerate to the right in order that no vacuum forms at the interface. A rarefaction traveling to the left through the air accomplishes just this.

Theoretical investigation of the limiting angles previously enumerated give the data presented in Fig. 15 for α_s, α_t, and α_i as a function of ξ. For a given ξ a reflected rarefaction is predicted for all values of α from 0 to α_t. At $\alpha=\alpha_t$ no reflected wave occurs at all. Between α_t and α_i the reflected wave is a shock and regular three-shock

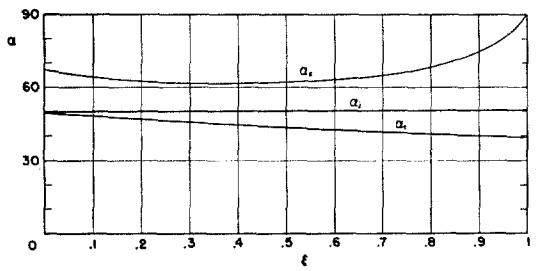

FIG. 15. Limiting angles on the regular refraction of shocks at an air-methane interface. For angles of incidence less than α_t theory predicts that the reflected wave is a rarefaction. Between α_t and α_i a reflected shock should occur, and above α_i no solution for regular refraction exists. In this case the requirement that the flow normal to the reflected wave R be supersonic is less severe than that given by α_i.

refraction should be observed. The interferogram shown in Fig. 16 verifies this prediction. When α_i is reached the outflowing methane becomes subsonic and the regular refraction pattern can no longer exist. Slightly beyond α_i the transmitted wave would run ahead and form some other pattern.

No theoretical approach has been made to such a situation so far but as may be seen from Fig. 17 the flow is quite complicated. At $\alpha=76°$ and $\xi=0.86$ the transmitted wave is considerably ahead of the incident wave and a signal has been retransmitted from the methane to the air. The incident and reflected waves have the appearance of Mach reflection except that the Mach stem is moving into a nonuniform region. In this case of an air-methane interface, the

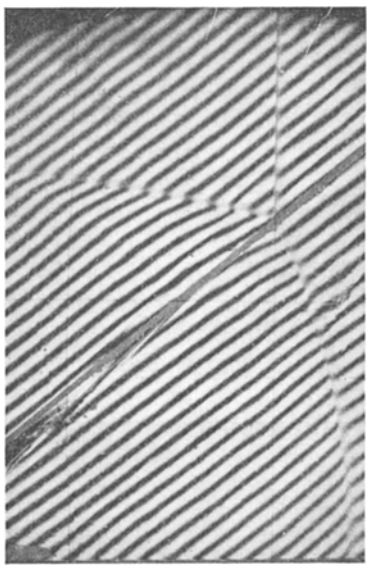

FIG. 16. Regular refraction of a shock at an air-methane boundary. $\xi=0.86$, $\alpha=51°$. Incident, reflected, and refracted shocks are visible. In this picture a thin film separates the two gases. The film is deflected downward by the shocks and a small gap may be seen between the film and holder behind the point of intersection. The ground plane is visible at the bottom of the picture.

limitation imposed by α_s and α_e are not reached. For other combinations of gases quite different patterns may be observed.

Diffraction, the third kind of shock interaction we shall discuss, bears even less similarity to its optical counterpart than do reflection and refraction because shocks have no wave nature (in spite of the common usage in calling them

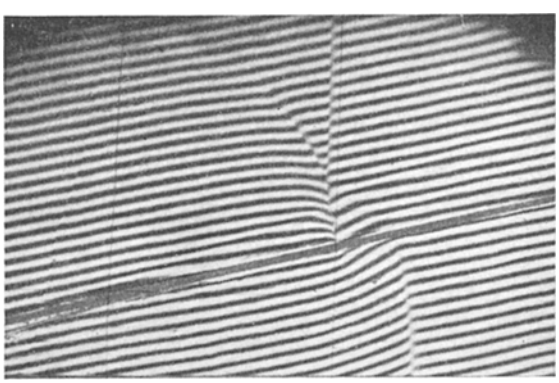

FIG. 17. Refraction at an air-methane interface with $\xi=0.86$, $\alpha=76°$. Here α is greater than the limiting angle α_i so that the transmitted shock has run ahead of the incident shock and retransmitted a compression wave into the air. Except for this disturbance the incident and reflected shocks are very like a Mach reflection in appearance.

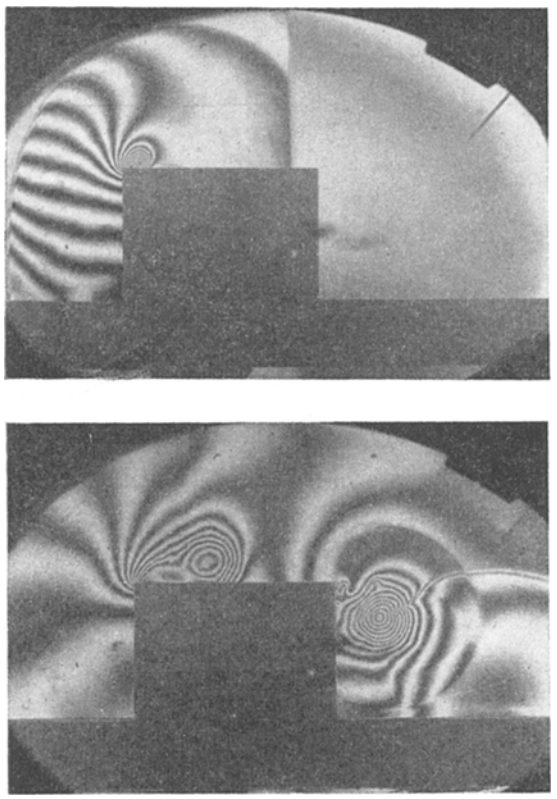

FIG. 18. Two stages in the diffraction of a shock over a rectangular block. The eddies formed behind each corner are regions of very low pressure. In the second picture the incident shock has reflected from the ground behind the block, entered the second eddy, been spun around clockwise, and come out as a nearly cylindrical shock.

shock waves) and therefore exhibit little of the phenomena of wave interference. Shock diffraction is important from the practical viewpoint these days for the engineer faced with the problem of the design of blast resistant structures. Not only is a structure suddenly immersed in an atmosphere of increased pressure when struck by a large blast wave but the shock front at the leading edge of the oncoming disturbance is diffracted about the object in a complicated manner setting up cross currents and eddies which profoundly affect the load distribution on the structure. Figure 18 shows two stages in the diffraction of a shock over a two-dimensional block in the shock tube. In the first picture the incident shock may be seen crossing the top of the block. A reflected shock travels to the left to inform the oncoming stream of the object's presence. An eddy forms behind the corner and is gradually swept downstream as it increases in size. The second shot shows how the incident wave reflects from the plane and is caught up in the eddy behind the block. Since a large clockwise circulation exists there the shock is spun around and emerges as a cylindrical shock. The interferogram may be evaluated in terms of the density and from these data the pressure can be calculated everywhere with considerable accuracy.[28,29] The pressures at the surface of the block give, of course, the force distribution (neglecting viscous effects) over the entire obstacle at this particular time. A series of such pictures allows the loads to be determined as a function of time. As the transient effects disappear one would expect the pressure loading on the block to approach that observed in wind tunnels. This is indeed the case.

Several other examples of diffraction are shown in Figs. 19, 20, and 21. There is no adequate theory for such phenomena. A considerable amount of experimental data has therefore been collected giving information about the pressure loading on a wide variety of objects.[28,29]

Space does not permit a discussion of all shock-wave interaction phenomena. For instance a considerable amount of work has been done on one-

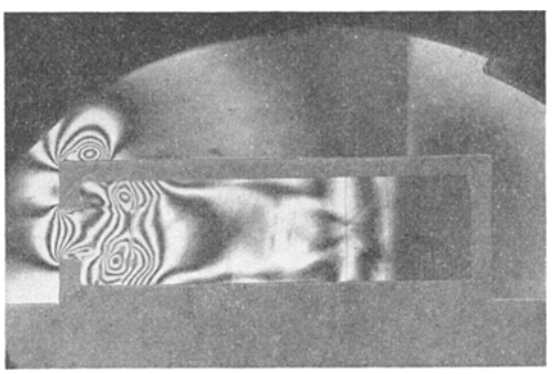

FIG. 19. Early stages in the filling of a hollow block after it has been struck by a shock. The net force on the top of the block is downward; later an upward force is observed when the shock inside reflects from the back wall.

[28] Bleakney, White, and Griffith, J. Appl. Mech. **17**, 439 (1950).

[29] W. Bleakney, "A shock tube investigation of the blast loading of structures," Proceedings of the Symposium on Earthquake and Blast Effects on Structures, University of California, Los Angeles, p. 46, 1952.

dimensional interactions.[11] Here theory and experiment are in good accord.

SHOCK STRUCTURE

A further goal in fluid dynamics is to understand the mechanisms that determine the thickness and structure of a shock. One might ask, for instance, whether the equations of a continuous fluid apply or not. If they do then viscosity and heat conduction are certainly important in the theory of shock structure because velocity and temperature gradients must be very high within the shock. The conservation equations for one-dimensional steady flow assume the form

$$(d/dx)\rho v = 0, \tag{13}$$

$$\frac{d}{dx}\rho v^2 + \frac{dp}{dx} - \frac{4}{3}\mu\frac{d^2v}{dx^2} = 0, \tag{14}$$

$$\rho v\frac{d}{dx}\left(h + \frac{v^2}{2}\right) = \frac{d}{dx}\kappa\frac{dT}{dx} + \frac{2\mu}{3}\left[2\left(\frac{dv}{dx}\right)^2 - v\frac{d^2v}{dx^2}\right], \tag{15}$$

where μ and κ are the coefficients of viscosity and thermal conductivity, respectively. Becker[30] first succeeded in solving the equations but made the assumption that these two coefficients are constant. Thomas[31] pointed out that Becker's result must be incorrect for strong shocks where the dependence of μ and κ on temperature is important. Using the kinetic theory result that both μ and κ vary as $\sqrt{T}$, Thomas obtained shock thicknesses considerably greater than those from the Becker theory. Nevertheless, since the values found are only a few mean free paths for shocks faster than $M \sim 1.2$, continuous fluid theory may not give as satisfactory an interpretation as the kinetic theory of gases.

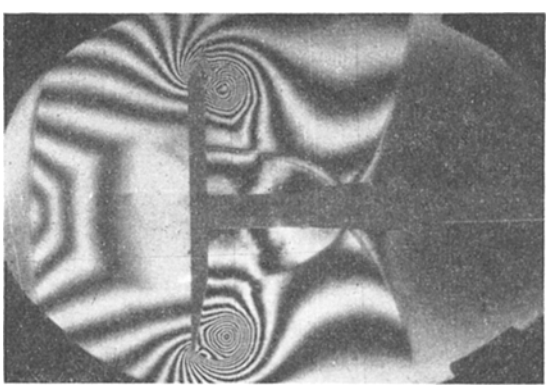

FIG. 20. Diffraction past a thin plate mounted perpendicular to the direction of shock travel. In this experiment one end of the plate was ground to a sharp edge to see what change this would make in the pattern. Very little effect can be seen.

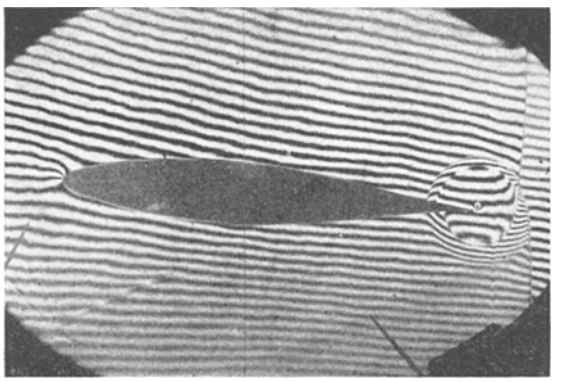

FIG. 21. A weak shock passing over an airfoil at a small angle of attack. The shock below the wing arrived at the rear first. Thus the diffracted part above the tail and the rarefaction which started downward simultaneously are a bit ahead of the rarefaction and shock, respectively, formed when the shock above the wing arrived at the rear. A small vortex may be seen a short distance behind the trailing edge.

Two rather distinct lines of approach have been taken in applying the kinetic theory to shocks. In one, successive approximations to a Maxwell-Boltzmann distribution

$$f_0(v_x, v_y, v_z) = (m/2\pi kT)^{\frac{3}{2}} \times \exp[-m(v_x^2+v_y^2+v_z^2)/2kT] \tag{16}$$

of molecular velocities are made by taking into account the effect of nonuniform conditions along the x direction.[32]

$$f = f_0 + f_1 + f_2 + \cdots. \tag{17}$$

Each term is assumed to be a function only of those preceding it.

$$f_1 = f_1(f_0), \qquad f_2 = f_2(f_0, f_1), \qquad f_3 = f_3(f_0, f_1, f_2), \cdots.$$

Equations (13)–(15) may be derived by retaining only $f_0 + f_1$. Thus a calculation using only the

[30] R. Becker, Z. Physik **8**, 321 (1923).

[31] L. H. Thomas, J. Chem. Phys. **12**, 449 (1944). See also A. E. Puckett and H. J. Stewart, Quart. Appl. Math. **7**, 457 (1950).

[32] For a discussion of this method see S. Chapman and T. G. Cowling, *The Mathematical Theory of Non-Uniform Gases* (Cambridge University Press, Cambridge, 1939), Chap. 7.

first-order terms would give just the Thomas theory again. Further terms from the expansion presumably improve the theory provided the solution converges rapidly enough to justify the assumption that the molecular velocity distribution may be obtained from Eq. (17) at all. Zoller[33] has carried out calculations to the third order on the variation of properties through shocks of pressure ratio $p_2/p_1=1.5$, 4, and 6.5. For the strongest shock $p_2/p_1=6.5$, the third-order terms are comparable in size to the first and second so that the accuracy of this solution is still in question. For $p_2/p_1\leq 4$ Zoller's results appear to be satisfactory.

Since shocks appear to get thinner with increasing Mach number Mott-Smith[34] has made the interesting suggestion that the velocity distribution may be composed of a mixture of two Maxwellian distributions corresponding to uniform conditions on the high- and low-temperature sides of the shock. Appreciable numbers of molecules from these two populations penetrate to the center of the shock. The structure itself is found by solving Boltzmann's equation[32] for the transport of kinetic energy across the shock.

A comparison of the various theories may be made by giving the shock thickness L as a function of Mach number. The quantity L is defined by the construction in the insert in Fig. 22 where it is seen to be the distance between intercepts of a tangent drawn at the steepest point of the shock profile. Very little difference exists in the shape of this profile in the various theories so no attempt is made to distinguish among them in comparing thicknesses. The parameter chosen as ordinate in Fig. 22 is Maxwell's mean free path λ in the gas ahead of the shock divided by shock thickness L.

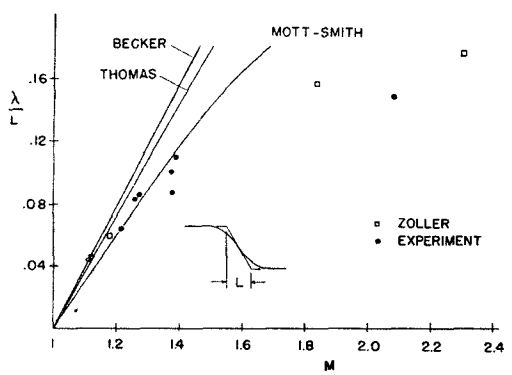

FIG. 22. Shock thickness L as a function of Mach number M. λ is Maxwell's mean free path. The circles are experimental points for argon obtained by Greene and Hornig. L is defined in the inset.

Owing to the extreme thinness of shocks only a little experimental data can be reported so far. Cowan and Hornig[35] have devised a method of measurement based on the reflectivity of a shock front. The amount of light reflected depends on the wavelength of the light, its angle of incidence, the index of refraction of the gas, the shock thickness, and its density profile. Measurements have been made in argon and nitrogen up to $M=2$.[36] The experimental points for argon are plotted on Fig. 22. Apparently the Mott-Smith and Zoller theories come closest to these experiments.

When molecules have rotational and vibrational energy as well, the picture becomes more complicated for, as has been known for a long time, exchange of kinetic energy with internal degrees of freedom takes place rather slowly. In nitrogen, for example, the average number of collisions to attain rotational equilibrium is slightly larger than the number in a weak shock front so that the foregoing theories are not directly applicable. In carbon dioxide at STP about twenty collisions are required on the average to exchange rotational quanta while 80 000 are needed for vibration. One might assume in this case that the shock consists of a narrow zone in which translation and rotation reach equilibrium followed by a region where vibrational energy comes slowly into adjustment.

Since the approach to vibrational equilibrium in carbon dioxide is spread out over such a large number of collisions it is possible to observe this lag with the interferometric techniques already described. Figure 23 shows a shock of Mach number 1.134 traveling through CO_2 at 200 mm Hg pressure and 23.5°C. An initial jump in density across the shock front is followed by a

[33] K. Zoller, Z. Physik, **130**, 1 (1951).
[34] H. M. Mott-Smith, Phys. Rev. **82**, 885 (1951).
[35] G. R. Cowan and D. F. Hornig, J. Chem. Phys. **18**, 1008 (1950).
[36] E. F. Greene and D. F. Hornig, "The shape and thickness of shock fronts in argon, hydrogen, nitrogen, and oxygen," ONR Contract N7onr-358, Tech. Rep. No. 4, Brown University, 1952.

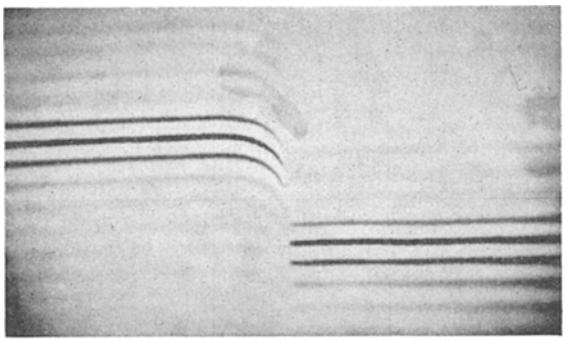

FIG. 23. A shock of Mach number 1.134 in CO_2. The region where vibrational energy gradually approaches equilibrium may be clearly seen. The two vertical hairlines are 1 in. apart. Data are given in Table II.

region of adjustment in which the density asymptotically approaches a final equilibrium value.

Bether and Teller[37] have given a theoretical treatment which may be used to interpret these effects. Conditions at state 2, immediately behind the shock front, may be found from Eqs. (4), (9), (10) with the assumption that only the vibrational energy remains unchanged in crossing the shock front. At 23.5°C, the specific heat at constant volume for CO_2 is divided among the various degrees of freedom as follows: $(3/2)R$ in translation, R in rotation (CO_2 is a linear symmetric molecule), and $0.95R$ in vibration. The appropriate specific heat ratio γ for calculating conditions at state 2 is therefore 1.4 and the effective Mach number is equal to the shock speed divided by the velocity of sound computed not counting the vibrational contribution to specific heat. The final equilibrium state 3 is found from Eqs. (5)–(7) taking into account the temperature dependence of enthalpy. Table II gives the values of pressure ratio, temperature, density ratio, and velocity in the three regions of Fig. 23. In their paper Bethe and Teller show that the values of velocity, density, etc., on the high-pressure side of the shock are uniquely determined by the initial conditions on the low-pressure side of the shock without reference to any of the intervening processes. It follows that the only effect of lagging heat capacity on a plane steady shock is to increase its thickness and not to alter the final state of the gas.

If one assumes that the vibrational state may be characterized by a temperature T_{vib} then the approach to equilibrium is governed by the relation

$$dc_{\text{vib}}T_{\text{vib}}/dt=(c_{\text{vib}}(T-T_{\text{vib}})/\tau), \qquad (18)$$

where c_{vib} is the vibrational specific heat and τ is the relaxation time. After a time τ the temperature difference would diminish to $1/e$, or 0.368, of its initial value in a case where the temperature change was small so that τ and c_{vib} remained constant. A fair estimate of τ may be made from Fig. 23 by measuring the distance d to the point where a given fringe has approached to within $1/e$ of its final position. The relaxation time is $\tau=d/v_2=11$ μsec. We have neglected the changing velocity and temperature as the gas flows away from the shock front and have assumed that the density also decays exponentially. Correcting for these factors makes only a small change in τ. Actually the CO_2 contains some impurities which, if eliminated, would make the relaxation time even longer.

Some experiments have been made on very strong shocks where a considerable fraction of the molecules receive enough energy to produce dissociation, electronic excitation, and ionization. A shock of Mach number 5 in argon, for example, is luminous over a region somewhat less than 100 mean free paths.[13] Other interesting effects have been observed with cylindrically converging shocks[38] and shocks produced in gaseous discharge tubes.[39] Since the energy of a converging shock is distributed among a continually decreasing number of particles, the possibility arises of producing exceedingly high temperatures. Esti-

TABLE II. Gas properties for the shock in carbon dioxide shown in Fig. 23. Region 1 is ahead of the shock, 2 immediately behind the shock front, and 3 far enough away for complete equilibrium to exist.

Region		1	2	3
Temperature	°C	23.5	40.7	43.0
Pressure ratio	p/p_1	1	1.214	1.359
Density ratio	ρ/ρ_1	1	1.148	1.276
Flow velocity	ft/sec	1014	883	795

[37] H. A. Bethe and E. Teller, "Deviations from thermal equilibrium in shock waves," Reissued by University of Michigan, Engineering Research Institute, Ann Arbor, 1951.

[38] R. W. Perry and A. Kantrowitz, J. Appl. Phys. **22**, 878 (1951).

[39] Fowler, Goldstein, and Clotfelter, Phys. Rev. **82**, 879 (1951).

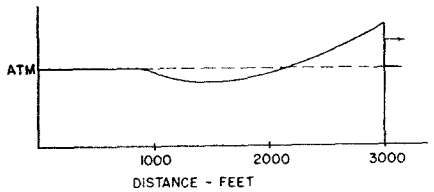

FIG. 24. Sketch of the pressure distribution 1.5 sec after the explosion of an atomic bomb. Atmospheric disturbances and the uneven ground greatly modify this idealized pattern at large distances.

mates of the temperature produced in this way have ranged well over 20 000°K. Luminous shocks have been produced in a tube by discharging a large condenser across it,[39] and spectral analysis of the light produced showed that He^{++}, N^{++}, and N^{+++} were present in the shock. Other measurements indicate that the duration of emission is not longer than one or two μsec. Many aspects of these phenomena have not been explained.

DECAY OF SHOCKS

In previous discussions of plane shocks in tubes we have assumed that immediately behind the front the flow variables were constant and the shock proceeded without attenuation. When the rarefaction reflected from the end of the chamber catches up with the shock this state of affairs is no longer true and the shock is rapidly attenuated. Even before this happens one cannot neglect completely the growth of boundary layers on the walls and the development of resistance to the flow which serves to slowly weaken the incident shock.[40] The effect decreases with increasing tube diameter.

The shock wave generated by an explosion or other concentrated source in a homogeneous atmosphere expands in three dimensions and decays very rapidly because of the ever greater area of its surface and the irreversible processes involved. The hot gases over expand creating a rarefaction which eats away the shock from behind giving it the peaked character commonly observed.[41] Figure 24 is a sketch of the state of affairs 1.5 seconds after the explosion of an atomic bomb of the "Able" type.[41] At a distance of 3000 feet the shock creates a pressure rise of 8 psi. Two miles from the center the shock has dropped to 1 psi and looking at the tail of the rarefaction in this figure one observes that the wave ends with a rise in pressure and this part is propagated into the region of the trough where the velocity of sound is lower. Evidently these are the qualitative conditions required for shock formation and, indeed, for weak shocks of short duration[42] a stable wave form has been observed consisting of a rise in pressure through a shock followed by a linear fall to an equal pressure below atmospheric and ending in a shock returning the pressure to atmospheric again. These "N" waves are a logical result of the discussion of Fig. 1 for increased amplitudes. They are not observed, however, for very large explosions presumably because, at the great distances one must go from the source before the amplitude can be called small, the durations become very long and the slope of the pressure-distance curve is below the value necessary for rapid shock growth. As a matter of practice in the field, the classical shape indicated in Fig. 24 is never observed for weak blast waves at great distances since the atmosphere is far from uniform and the earth is not an ideal boundary. From thirty to several hundred miles the refractive effects of temperature gradients and wind currents lead to interfering effects from multiple paths which result in widely distorted sound waves of large amplitudes[43] but low fundamental frequencies of the order of one fifth cycle per second.

[40] R. J. Emrich and C. W. Curtis, J. Appl. Phys. **24**, 360 (1953).

[41] U. S. Atomic Energy Commission, *The Effects of Atomic Weapons* (McGraw-Hill Book Company, Inc New York 1950).

[42] DuMond, Cohen, Panofsky, and Deeds, J. Acoust. Soc. Am. **18**, 97 (1946).

[43] E. F. Cox, J. Acoust. Soc. Am. **19**, 832 (1947).

Concerning new discoveries and theories, Thomas Young says, "The discovery of simple and uniform principles, by which a great number of apparently heterogeneous phenomena are reduced to coherent and universal laws, must ever be allowed to be of considerable importance toward the improvement of the human intellect."—Thomas Young, Natural Philosopher by ALEX WOOD (Cambridge University Press, 1954).

The above may be an example of Thomas Young's verbose and heavy prose by which he failed to be a clear lecturer.—ED.